Does TARDIS do what it does fast enough?

Caroline Sofiatti

June 5, 2014

Contents

1 Introduction

Type Ia supernova (SN Ia) modeling has greatly evolved since the first one-dimensional SN model created in the early 80's [8]. Today, full explosion models such as ARTIS [4]

and SEDONA [2] are the state-of-the-art and present a much more complete but complex representation of SNe. Such robustness comes at the expense of execution time, even with parallelism. These models are too costly to use directly in large parameter-space studies. TARDIS (see [3]) attempts to address this problem.

2 About TARDIS

TARDIS is an open-source code for rapid modeling of SN spectra. The code uses indivisible energy-packet Monte Carlo (MC) methods [1] [5] [6] to obtain a description of the SN's plasma state and to compute a synthetic spectrum.

Unlike SYNAPPS [9], a simple approach for spectral line identification, TARDIS is an analysis tool that attempts to balance accuracy and computational expense according to the needs of a specific study. It is based on the same methods used by ARTIS, but users should keep in mind that TARDIS is much more limited. Finally, TARDIS uses the YAML markup language for its configuration files. An example of a configuration file follows in appendix A.

2.1 Configuration File

A TARDIS configuration file is organized into three main sections: `model` - where the density profile and the elemental abundances are set, `plasma` - where plasma conditions such as ionization and excitation can be fixed, and `montecarlo` - where the settings for the MC are established.

2.1.1 Model

A TARDIS model is spherically symmetric. The computational domain is discretized into multiple spherical shells. For each of these shells, the density and elemental abundances must be specified. The `model` section of the TARDIS configuration file contains two subsections: `structure` and `abundances`.

The `structure` subsection determines the density profile of the SN through the `density` parameter. The default on the original YAML file is set to `branch85_w7`. This is a density profile based on a simple fit (ρv^{-7}) to the W7 model of Nomoto et al. [7]. Nevertheless, an arbitrary density can be included, if required. This can be achieved by setting the abundance parameter `type` to `file` and including an arbitrary density profile as an ASCII file.

The `abundances` section is set as uniform on the original YAML file. Similarly to `density`, `abundance` can include stratified elemental abundances. This can be done by changing `type` to `file` and including an ASCII file that specifies the abundances for each shell.

2.1.2 Plasma

TARDIS currently supports three different types of line interaction: `macroatom`, `downbranch` and `scatter`. Macro-atoms [5] are a conceptual construct that facilitates the derivation and implementation of the MC transition probabilities. They contribute to an accurate treatment of the line interaction. More specifically, macro-atoms are a quanta of matter

whose properties are such that their interactions with energy packets (see § 2.1.3) asymptotically reproduce the reprocessing of radiation by macroscopic volume elements of a gas that is in statistical and radiative equilibrium. Additionally, the line interaction can be treated approximately, assuming either resonant scattering or downward branching following absorption.

TARDIS also allows the user to enable or disable electron scattering. Disabling scattering is mostly used for debugging purposes and to compare results to SYNAPPS (see fig. 4).

Also, there are currently two ionization options: `LTE`, which calculates the ionization fractions from the Saha-Boltzmann equation, and `nebular`, which calculates the ionization fractions from the nebular approximation explained by Equation 3 in [3](see fig. 3).

Finally, the excitation modes can be `LTE` or `dilute LTE`. `LTE` calculates level populations from the Boltzmann equation and `dilute LTE` uses reduced excited level populations (see fig. 2).

2.1.3 Montecarlo

TARDIS is an implementation of the energy-packet MC. According to this formalism [1] [5] [6], packets are indivisible, monochromatic quanta of radiant energy. This constraint is used because it leads to a simple code.

The MC radiation field is generated iteratively to compute the radiative equilibrium temperature stratification and one can specify a different number of packets for the last MC simulation. Though the boundary temperature T_b is iteratively improved, in the final iteration T is established and the spectrum is computed. We will discuss in § 5.2 how the number of packets in the last iteration affects the signal-to-noise ratio (S/N) of the final spectrum.

Also during this last simulation, a set of test packets referred to as virtual packets are created. These packets serve to reduce variance.

One can set the number of packets, last packets, and virtual packets in the `montecarlo` section.

2.2 Future versions of TARDIS

According to [3], in the near future TARDIS will incorporate additional physics such as bound-free/ thermalization processes for a more sophisticated ionization approximation and to allow for spectral synthesis of SNe II. Another future implementation is to compute opacities to handle radiation-matter interactions.

2.3 About this report

This report aims at introducing TARDIS and at analyzing its performance in order to characterize the tradeoff between quality of fits and execution time for a run. With this information, potential SNfactory users will be able to determine which settings they should pick when considering a high quality publication plot or a fast exploratory run.

We conduct an exectution time vs. S/N trade study as follows: We start with the original configuration file then varied the number of packets, last packets, and virtual packets, since

these variables significantly impact the noisiness of the output. We then repeated this for three different line interation settings: `macroatom`, `downbranch` and `scatter` (see 4). The same procedure was extended to three other settings configurations that are slight modifications from the original, for the sake of comparison. See table 2.

We compare the spectrum to a very high S/N spectrum in order to obtain a value for the noise and we extract the execution time of the run from the TARDIS log file.

- All the runs have the same configuration as the original TARDIS YAML file that follows in the appendix (see appendix A). The same uniform abundance profile is used throughtout this study. This abundance profile follows in table 1. Moreover, for each case, only the YAML entry under investigation was changed unless otherwise specified.

- TARDIS creates spectra from 500Åto 20000Å. In this report, I only use information contained in the range from 3000Åto 10000Å, since this is the range of a typical SNfactory spectrum in the rest frame.

- The reference spectrum is computed with 10^7 packets, 10^7 last packets and 100 virtual packets (essentially infinite S/N). See fig. 1. Note that this spectrum is UV bright for a SN Ia. In order to achieve a more realistic simulation, the TARDIS configurations have to modified. We expect the execution times to be higher for a more realistic simulation, because of less line blanketing in the UV. Nevertheless, the S/N ratios should remain the same. Therefore, the results presented in this report will still be valid.

- Noise is the residual luminosity of one spectrum relative to the reference spectrum divided by the mean luminosity of the reference spectrum.

Element	Abundance
O	0.19
Mg	0.03
Si	0.52
S	0.19
Ar	0.04
Ca	0.03

Table 1: Uniform Abundance Settings

2.3.1 Cases I - IV

Cases I-IV represent a set of fixed values as described in table 2. Case I represents the settings of the original configuration file. Case II is a slight modification from case I, where the number of packets and last packets increase by order 10. The number of virtual packets is set to zero. Similarly, case IV is obtained by decreasing the settings of case I by order 10. Cases II and III differ only by number of virtual packets. This allows us to isolate the effect of increasing the number of virtual packets.
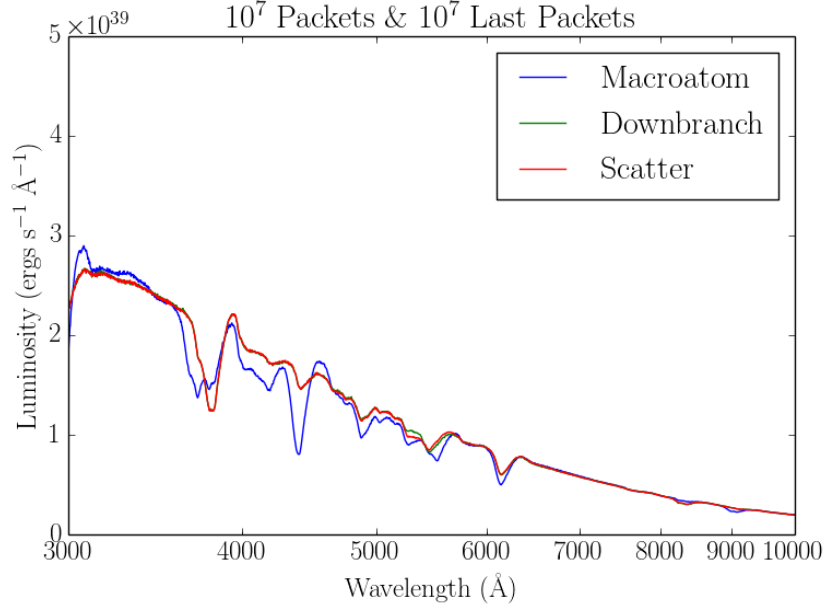
Figure 1: Reference simulation spectra. The number of virtual packets is 100. Time since explosion is 13 days.

Case	Packets(10^3)	Last Packets (10^4)	Virtual Packets
I	40	10	10
II	400	100	0
III	400	100	10
IV	4	1	10

Table 2: Settings configuration for cases I-IV

2.3.2 About my computer

All the runs contained in this report were performed on a 2011 MacBook Pro with a 2.4 GHz Intel Core i5 processor and 4 GB 1333 MHz DDR3 memory. We consider the execution time to be the number of seconds printed on the last line of the TARDIS log file. E.g., `tardis.simulation – INFO – Finished in 20 iterations and took 40.23 s.`

3 Plasma: analyzing spectra

As of today, four of the variables in the plasma section can be changed. The line interation type can be `macroatom`, `downbranch` or `scatter` as illustrated by the previous figures in this report. The excitation can be either `LTE` or `dilute LTE` (see fig. 2). The ionization can be either `LTE` or `nebular` (see fig. 3) and electron scattering can be either enabled or disabled (see fig. 4).
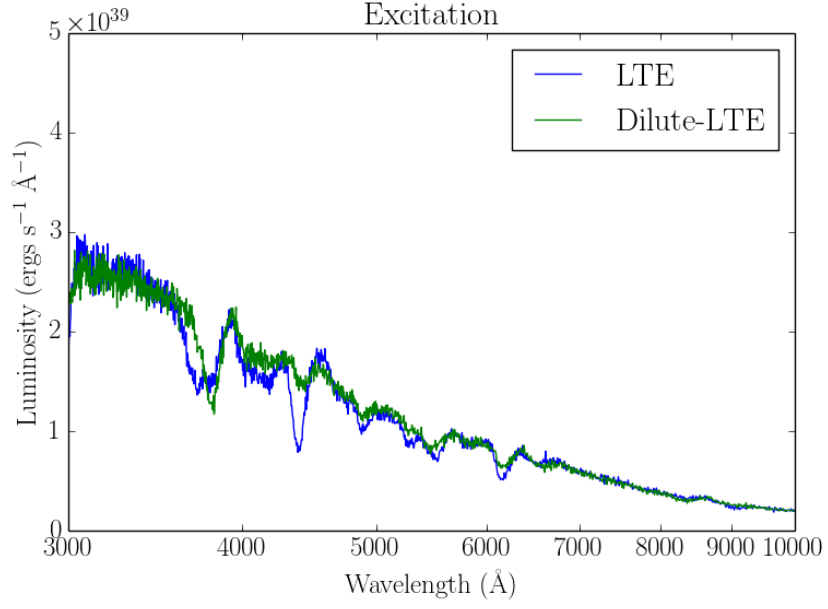
Figure 2: Typical difference in spectrum between `LTE` and `Dilute LTE` excitation. Fixed values: Number of packets is 4×10^4, last number of packets is 10^5 and the number of virtual packets is 10. Line interaction type is macroatom and time since explosion is 13 days.

Figure 3: Typical difference in spectrum between `LTE` and `Nebular` ionization. Fixed values: Number of packets is 4×10^4, last number of packets is 10^5 and the number of virtual packets is 10. Line interaction type is macroatom and time since explosion is 13 days. Excitation is set to dilute LTE.
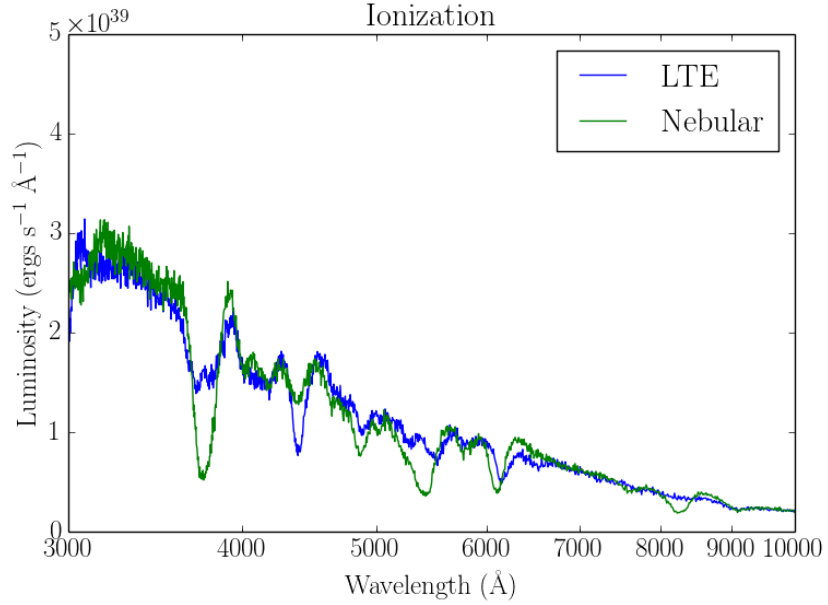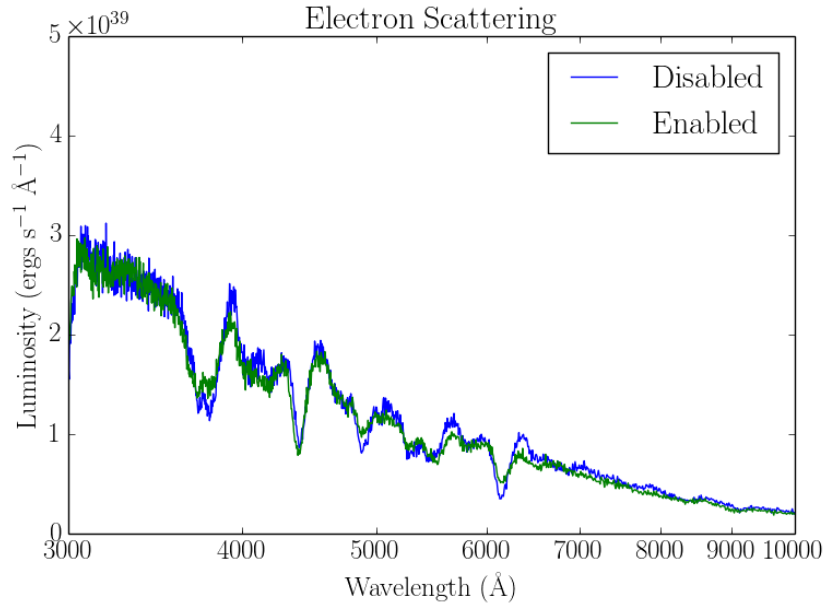
6

Figure 4: Effect of electron scattering. Fixed values: Number of packets is 4×10^4, last number of packets is 10^5 and the number of virtual packets is 10. Line interaction type is macroatom and time since explosion is 13 days.

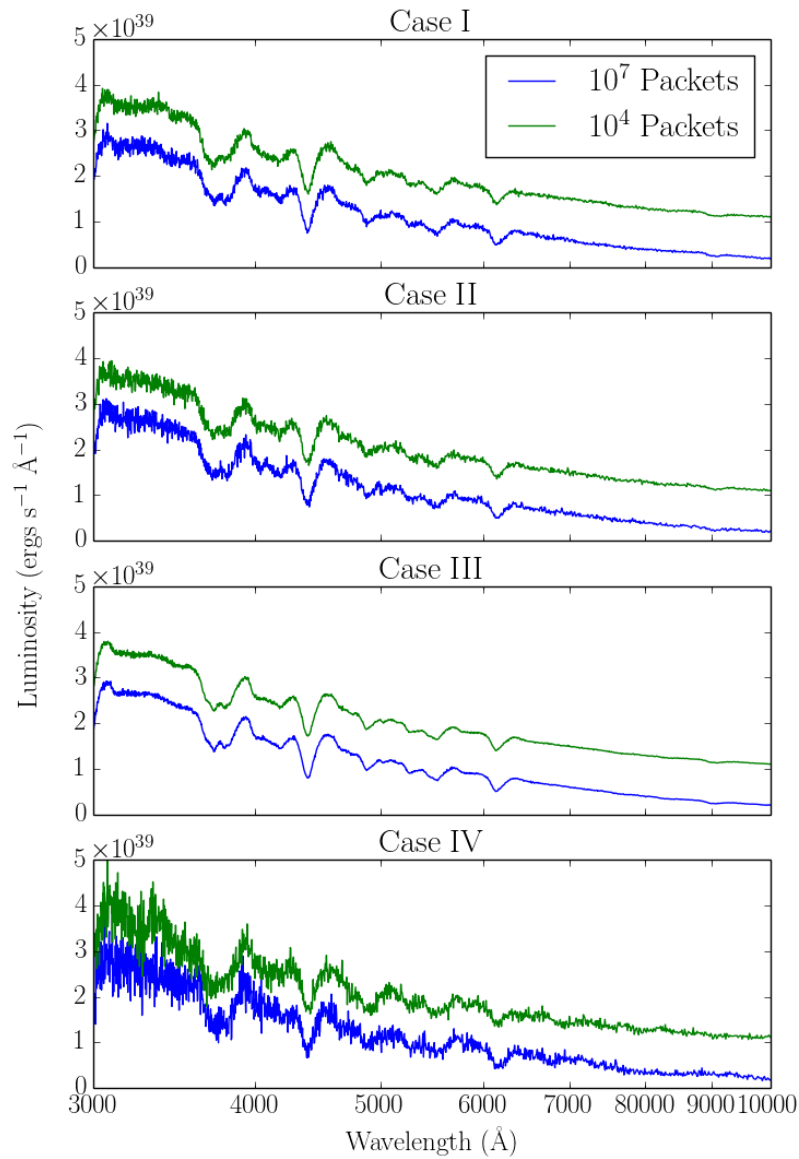# 4 Monte Carlo: analyzing spectra

4.1 Packets

Figure 5: Each subplot shows a pair of very similar spectra, indicating that 10^4 packets are sufficient for computing the radiative equilibrium temperature.

4.2 Last packets

Figure 6: Luminosity as a function of wavelength for 10^7 packets. The luminosity is offset for each case above case I. Time since explosion is 13 days.
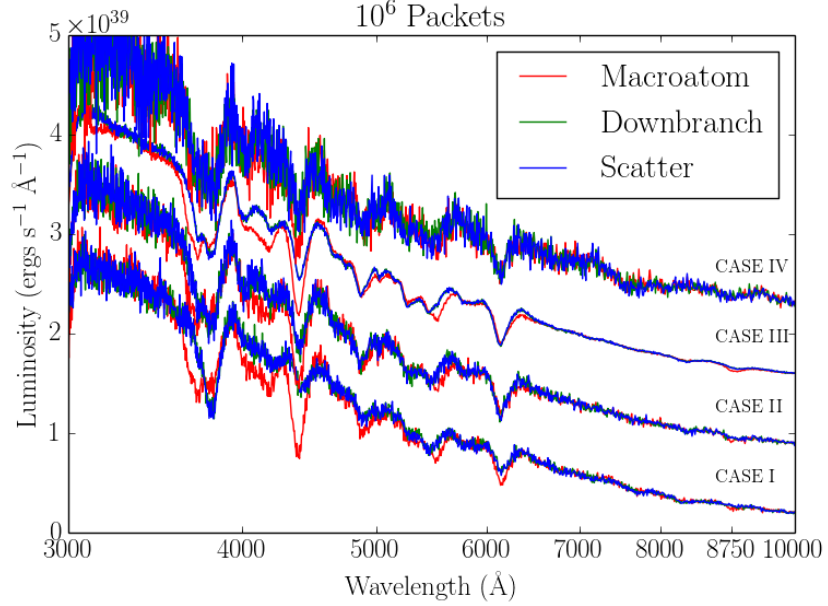
Figure 7: Luminosity as a function of wavelength for 10^6 packets. The luminosity is offset for each case above case I. Time since explosion is 13 days.
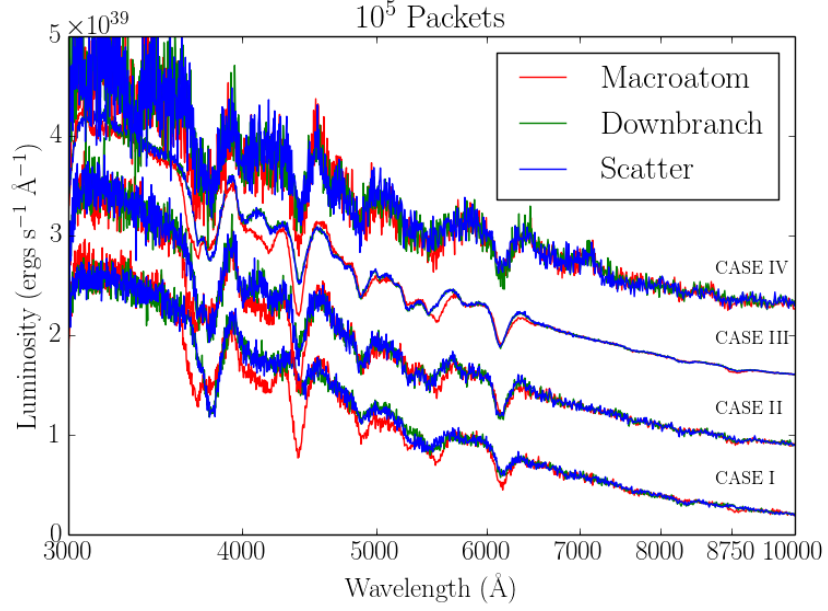
Figure 8: Luminosity as a function of wavelength for 10^5 packets. The luminosity is offset for each case above case I. Time since explosion is 13 days.
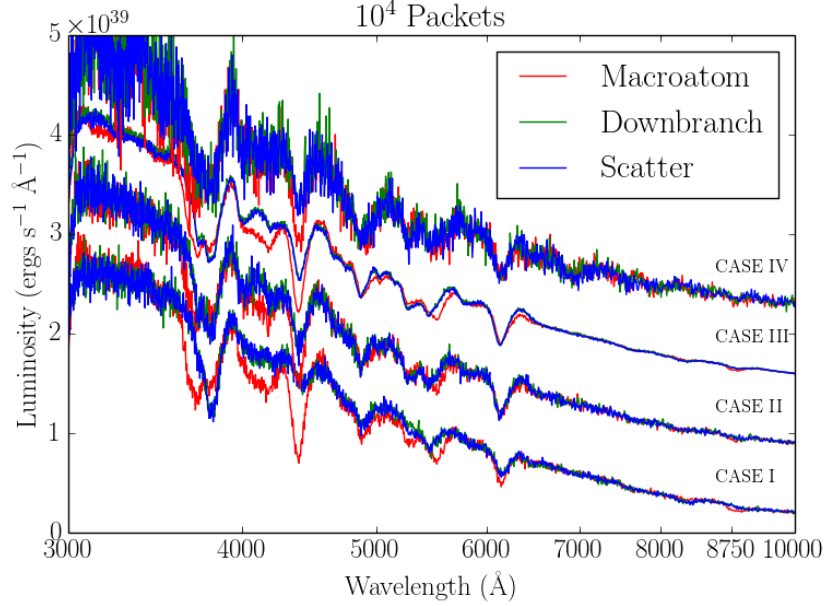
Figure 9: Luminosity as a function of wavelength for 10^4 packets. The luminosity is offset for each case above case I. Time since explosion is 13 days.
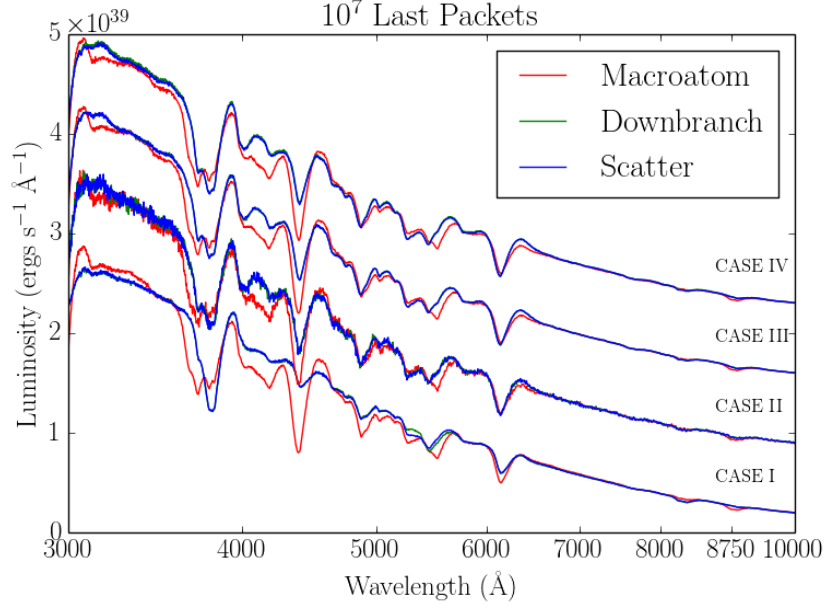
Figure 10: Luminosity as a function of wavelength for 10^7 last packets. The luminosity is offset for each case above case I. Time since explosion is 13 days.
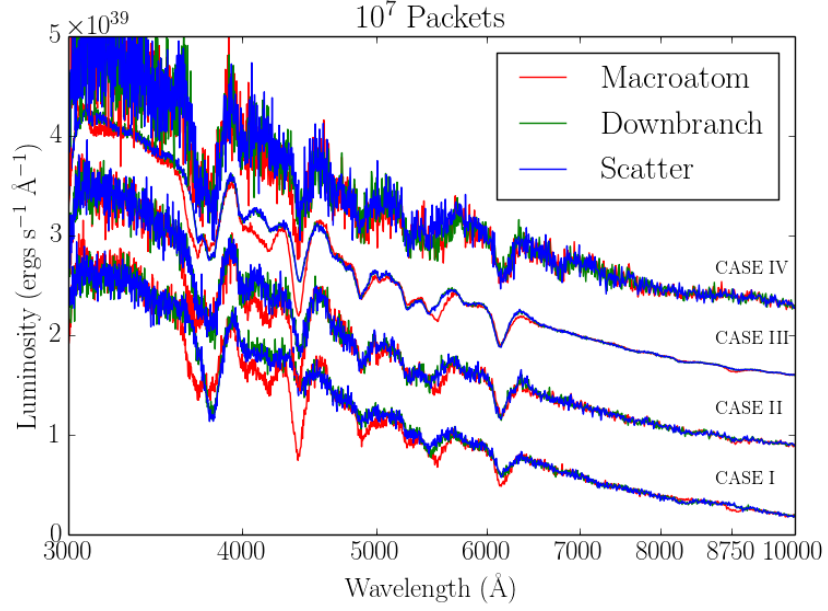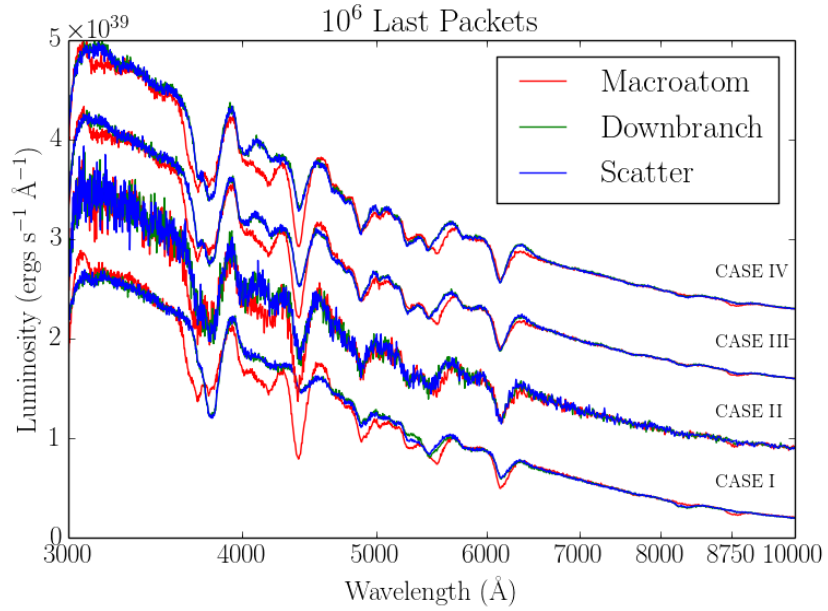

Figure 11: Luminosity as a function of wavelength for 10^6 last packets. The luminosity is offset for each case above case I. Time since explosion is 13 days.

Figure 12: Luminosity as a function of wavelength for 10^5 last packets. The luminosity is offset for each case above case I. Time since explosion is 13 days.

Figure 13: Luminosity as a function of wavelength for 10^4 last packets. The luminosity is offset for each case above case I. Time since explosion is 13 days.
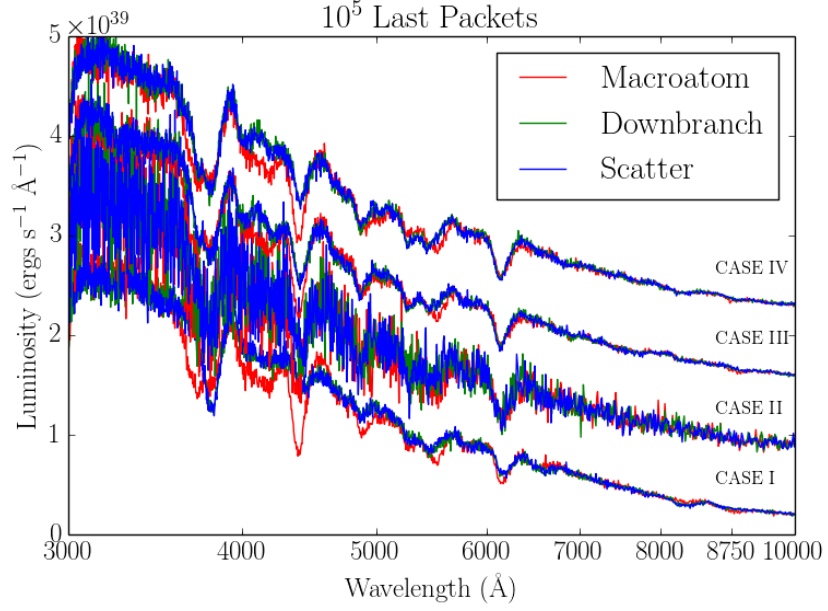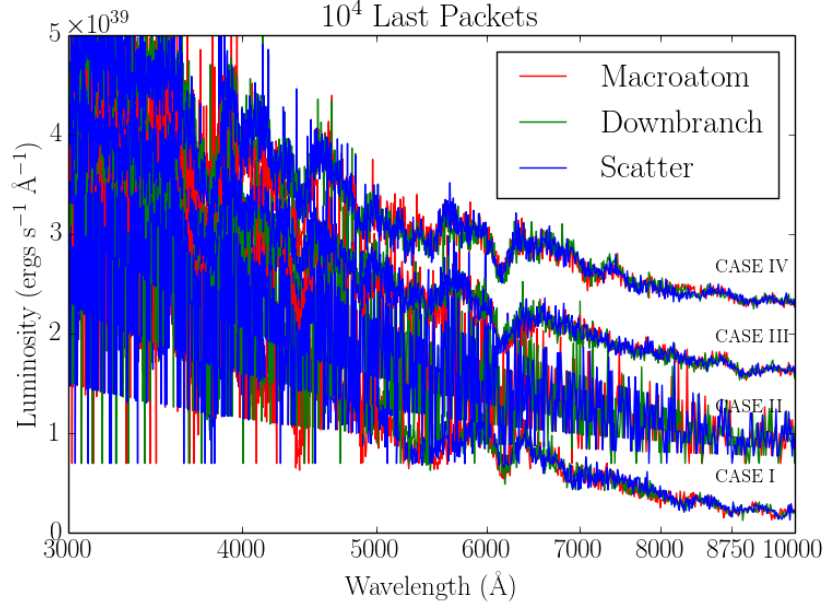
5 Monte Carlo: signal to noise

5.1 Packets

	Macroatom		Downbranch		Scatter	
Packets	t(s)	Noise	t(s)	Noise	t(s)	Noise
10^7	2990.52	0.109	15251.93	0.049	2991.03	0.048
10^6	322.09	0.118	299.39	0.046	330.66	0.051
10^5	57.85	0.116	65.45	0.049	52.99	0.045
10^4	34.20	0.126	31.79	0.050	30.71	0.049
10^3	**28.04**	**0.095**	**30.55**	**0.046**	**26.62**	**0.047**
10^2	28.76	0.161	27.91	0.071	27.05	0.063
10^1	28.20	0.389	27.78	0.097	27.41	0.141
Figure	14(a)		15(a)		16(a)	

Table 3: CASE I for number of packets. Fixed values: last number of packets is 10^5 and the number of virtual packets is 10. t(s) is the execution time in seconds. Noise is the normalized standard deviation (see discussion above). The best payoff is indicated by numbers in bold (see respective figure).

	Macroatom		Downbranch		Scatter	
Packets	t(s)	Noise	t(s)	Noise	t(s)	Noise
10^7	3260.99	0.122	3025.44	0.085	6256.71	0.089
10^6	360.16	0.121	330.81	0.086	356.91	0.089
10^5	**58.00**	**0.121**	**54.37**	**0.087**	**53.67**	**0.090**
10^4	29.04	0.117	**27.46**	**0.087**	**26.97**	**0.083**
10^3	25.87	0.114	26.26	0.086	24.10	0.091
10^2	27.56	0.143	24.41	0.097	26.08	0.087
10^1	26.72	0.399	24.74	0.123	24.15	0.098
Figure	14(b)		15(b)		16(b)	

Table 4: CASE II for number of packets. Fixed values: last number of packets is 10^6 and the number of virtual packets is 100. t(s) is the execution time in seconds. Noise is the normalized standard deviation (see discussion above). The best payoff is indicated by numbers in bold (see respective figure).

	Macroatom		Downbranch		Scatter	
Packets	t(s)	Noise	t(s)	Noise	t(s)	Noise
10^7	3317.59	0.107	3204.63	0.066	3453.88	0.065
10^6	534.01	0.108	481.55	0.065	560.64	0.066
10^5	212.11	0.107	230.55	0.066	270.44	0.066
10^4	184.32	0.106	**206.10**	**0.066**	**232.46**	**0.062**
10^3	**183.08**	**0.101**	**196.23**	**0.066**	**217.11**	**0.072**
10^2	187.15	0.130	189.80	0.078	213.09	0.068
10^1	181.13	0.388	194.59	0.114	190.78	0.077
Figure	14(c)		15(c)		16(c)	

Table 5: CASE III for number of packets. Fixed values: last number of packets is 10^6 and the number of virtual packets is 10. t(s) is the execution time in seconds. Noise is the normalized standard deviation (see discussion above). The best payoff is indicated by numbers in bold (see respective figure).

	Macroatom		Downbranch		Scatter	
Packets	t(s)	Noise	t(s)	Noise	t(s)	Noise
10^7	2889.75	0.179	2942.73	0.153	2780.58	0.150
10^6	306.79	0.179	289.60	0.162	290.00	0.169
10^5	41.88	0.176	38.89	0.159	42.60	0.158
10^4	**15.32**	**0.202**	**13.32**	**0.174**	**15.52**	**0.170**
10^3	**12.38**	**0.178**	**10.96**	**0.159**	11.79	0.173
10^2	12.55	0.221	**10.75**	**0.176**	**10.35**	**0.173**
10^1	12.68	0.395	**10.83**	**0.178**	**10.26**	**0.183**
Figure	14(d)		15(d)		16(d)	

Table 6: CASE IV for number of packets. Fixed values: last number of packets is 10^4 and the number of virtual packets is 10. t(s) is the execution time in seconds. Noise is the normalized standard deviation (see discussion above). The best payoff is indicated by numbers in bold (see respective figure).

5.2 Last packets

Last Packets	Macroatom t(s)	Macroatom Noise	Downbranch t(s)	Downbranch Noise	Scatter t(s)	Scatter Noise
10^7	2247.55	0.105	1589.88	0.010	1899.35	0.007
10^6	201.72	0.106	183.30	0.018	197.30	0.016
10^5	**44.77**	**0.113**	**42.24**	**0.049**	**40.08**	**0.048**
10^4	26.41	0.179	25.60	0.150	25.46	0.155
10^3	25.11	0.473	24.50	0.473	27.93	0.487
10^2	28.91	1.486	24.20	1.593	23.94	1.375
10^1	25.17	3.859	21.88	4.216	20.17	4.190
Figure	17(a)		18(a)		19(a)	

Table 7: CASE I for last number of packets. Fixed values: number of packets is 4×10^4 and the number of virtual packets is 10. t(s) is the execution time in seconds. Noise is the normalized standard deviation (see discussion above). The best payoff is indicated by numbers in bold (see respective figure).

Last Packets	Macroatom t(s)	Macroatom Noise	Downbranch t(s)	Downbranch Noise	Scatter t(s)	Scatter Noise
10^7	274.38	0.107	268.26	0.067	280.95	0.067
10^6	163.42	0.119	135.05	0.085	140.32	0.086
10^5	**136.37**	**0.200**	**122.11**	**0.188**	**125.27**	**0.192**
10^4	135.73	0.579	121.12	0.580	124.48	0.603
10^3	129.09	1.919	120.52	1.958	122.16	1.850
10^2	131.19	5.221	125.98	5.105	122.66	5.194
10^1	133.83	17.012	121.13	18.014	127.79	18.601
Figure	17(b)		18(b)		19(b)	

Table 8: CASE II for last number of packets. Fixed values: number of packets is 4×10^5 and the number of virtual packets is 100. t(s) is the execution time in seconds. Noise is the normalized standard deviation (see discussion above). The best payoff is indicated by numbers in bold (see respective figure).

	Macroatom		Downbranch		Scatter	
Last Packets	t(s)	Noise	t(s)	Noise	t(s)	Noise
10^7	1775.22	0.106	1744.39	0.064	1748.00	0.064
10^6	287.85	0.105	287.89	0.065	282.70	0.066
10^5	**139.57**	**0.116**	**138.05**	**0.079**	**135.33**	**0.081**
10^4	124.93	0.183	121.99	0.162	119.67	0.153
10^3	122.96	0.503	126.50	0.467	118.56	0.513
10^2	123.22	1.327	125.18	1.402	117.03	1.255
10^1	122.95	4.611	119.71	4.411	117.13	4.036
Figure	17(c)		18(c)		19(c)	

Table 9: CASE III for last number of packets. Fixed values: number of packets is 4×10^5 and the number of virtual packets is 10. t(s) is the execution time in seconds. Noise is the normalized standard deviation (see discussion above). The best payoff is indicated by numbers in bold (see respective figure).

	Macroatom		Downbranch		Scatter	
Last Packets	t(s)	Noise	t(s)	Noise	t(s)	Noise
10^7	1717.38	0.101	1786.01	0.063	1750.40	0.061
10^6	189.30	0.102	184.42	0.066	177.22	0.065
10^5	**30.55**	**0.107**	**27.95**	**0.076**	**27.25**	**0.073**
10^4	15.33	0.175	11.80	0.164	11.30	0.161
10^3	12.32	0.495	12.00	0.509	10.33	0.517
10^2	11.82	1.734	10.34	1.702	9.90	1.733
10^1	12.03	5.142	9.89	6.258	9.54	6.370
Figure	17(d)		18(d)		19(d)	

Table 10: CASE IV for last number of packets. Fixed values: number of packets is 4×10^3 and the number of virtual packets is 10. t(s) is the execution time in seconds. Noise is the normalized standard deviation (see discussion above). The best payoff is indicated by numbers in bold (see respective figure).
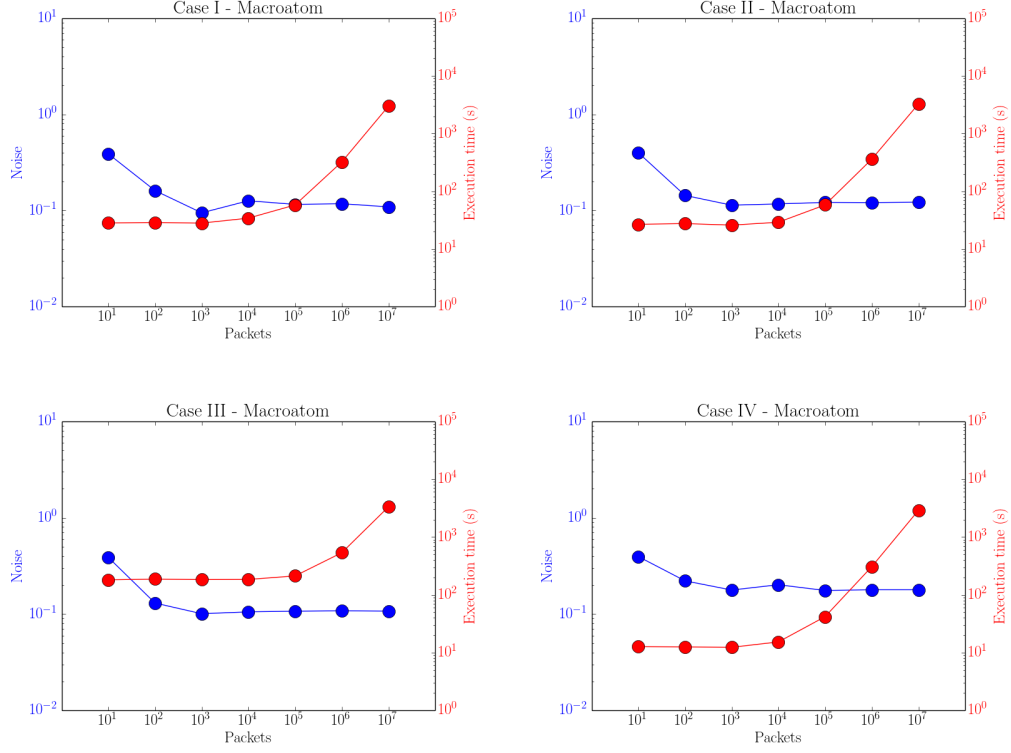
Figure 14: Noise and execution time as a function of packets for macroatom.

6 Conclusion

Virtual packets are not as relevant to yielding a low S/N as the number of last packets. We reach this by analyzing figs. 6- 9. In these figures, only virtual packets and last packets change from case to case. The fact that cases II and III have similar noise (though case III is slightly noisier) indicates that the number of last packets is the main determinant of the noise. Recall that cases II and III have the same number of last packets.

Moreover, fig. 10 shows that if the number of packets is high (above $\sim 10^7$), the number of packets and the number of virtual packets do not play an important role in determining the noisiness of the simulation. As the number of last packets decrease, figs 11, 12, and 13 show that the number of virtual packets are a better indicator of the noise than the number of packets. Finally, case IV of fig. ?? suggests that one can obtain spectra with a relatively low S/N even if the number of last packets and the number of packets are low ($\sim 10^5$ and $\sim 10^4$, respectively). Nevertheless, there is a loss of accuracy. Note that the spectrum for macroatom differs from the spectrum for downbranch more noticeably than in the other plots.

Finally, optimal settings for the number of packets, last packets and virtual packets, are inferred from tables 3- ??. The most occurring values are summarized in table 11.
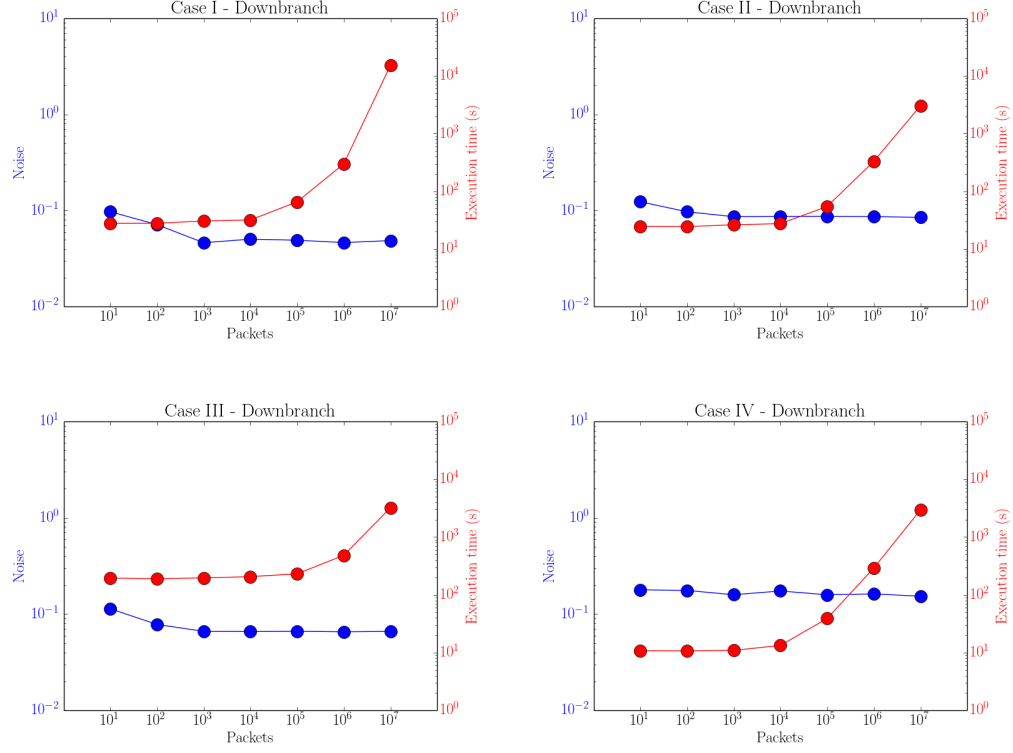
17

Figure 15: Noise and execution time as a function of packets for downbranch.

	Case I	Case II	Case III	Case IV
Packets	10^3	10^3	10^3	10^4
Last packets	10^5	10^4	10^5	10^5

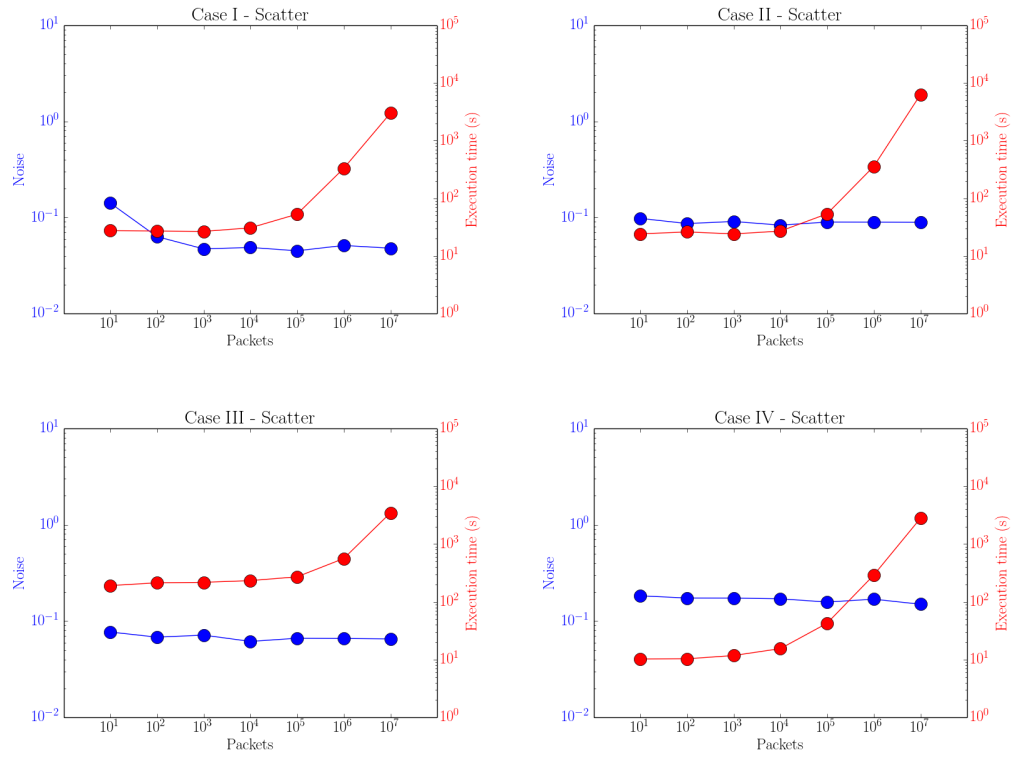Table 11: Optimal settings configuration for cases I-IV

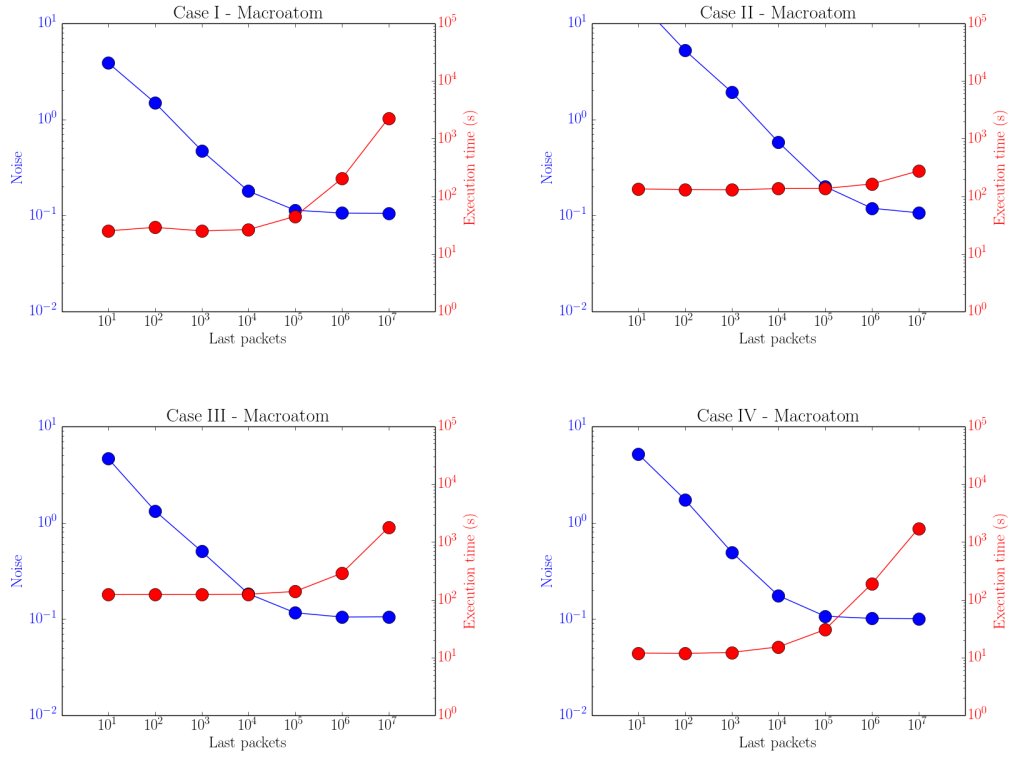Figure 16: Noise and execution time as a function of packets for scatter.

Figure 17: Noise and execution time as a function of last packets for macroatom.
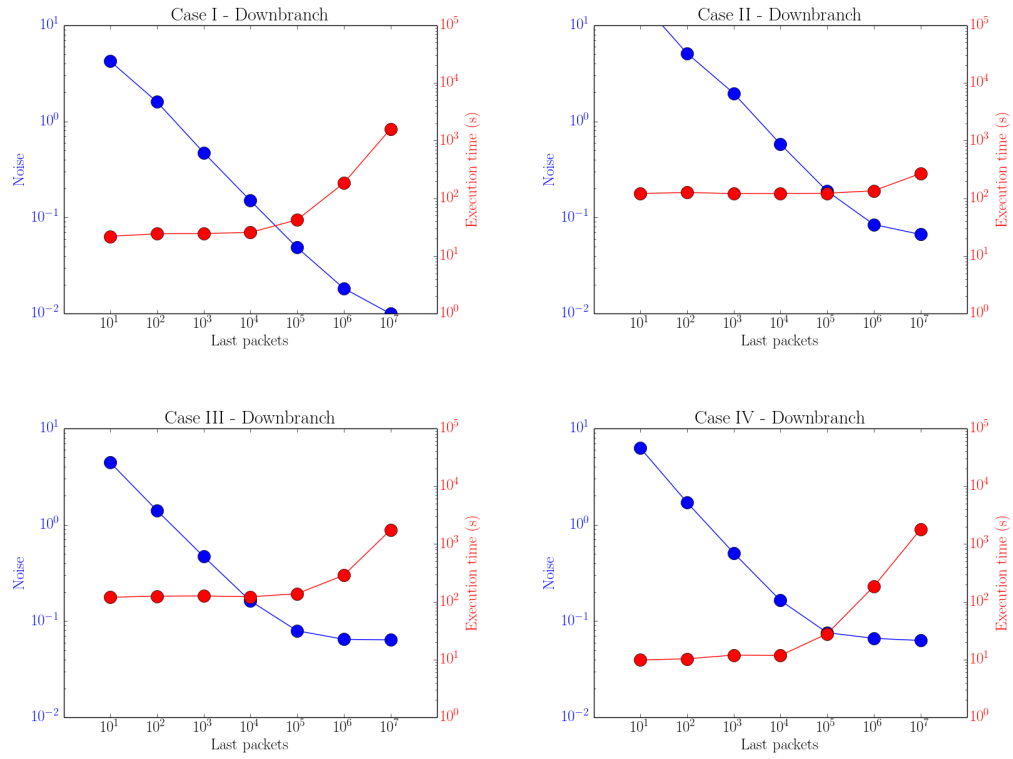
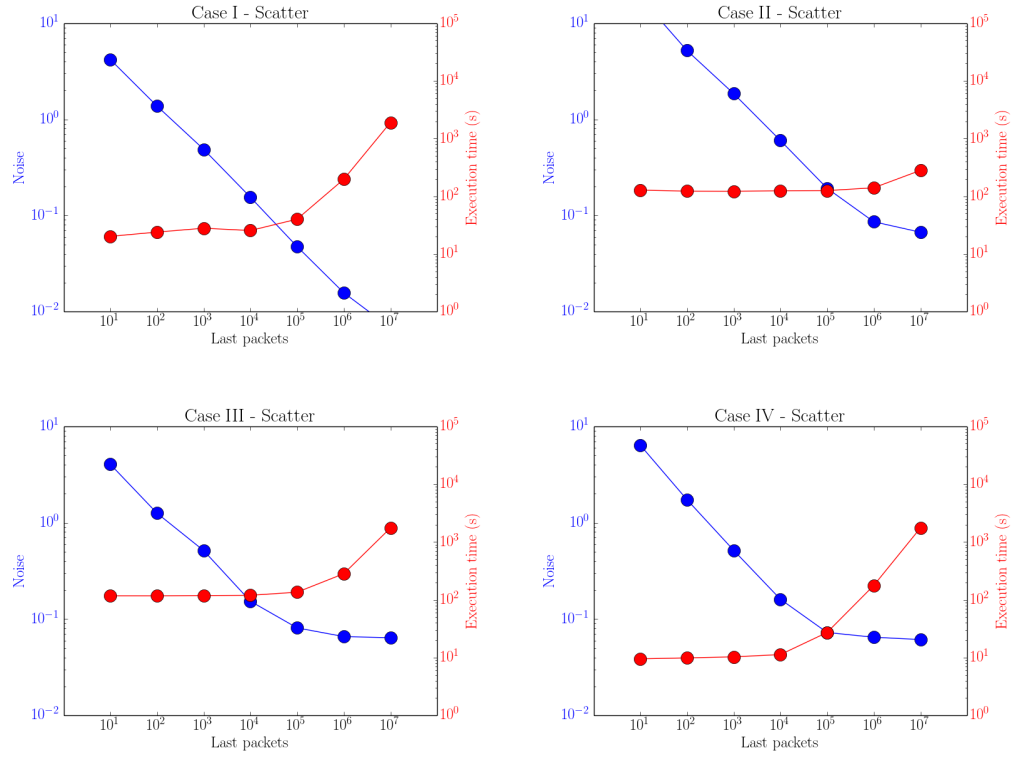Figure 18: Noise and execution time as a function of last packets for downbranch.

Figure 19: Noise and execution time as a function of last packets for scatter.

Appendices

A Original YAML file

```
#New configuration for TARDIS based on YAML
#IMPORTANT any pure floats need to have a +/- after the e e.g. 2e+5
#Hopefully pyyaml will fix this soon.
---
#Currently only simple1d is allowed
tardis_config_version: v1.0
supernova:
   luminosity_requested: 9.44 log_lsun
   time_explosion: 13 day
#   distance : 24.2 Mpc


atom_data: kurucz_atom_pure_simple.h5


model:


   structure:
      type: specific


      velocity:
         start : 1.1e4 km/s
         stop : 20000 km/s
         num: 20


      density:
         #showing different configuration options separated by comments
         #simple uniform:
         #--------------
         #type : uniform
         #value : 1e-40 g/cm^3
         #--------------

         #branch85_w7 - fit of seven order polynomial to W7 (like
            Branch 85):
         #--------------
         type : branch85_w7

         # default, no need to change!
```

```
        #time_0 : 19.9999584 s
        # default, no need to change!
        #density_coefficient : 3e29
        #---------------


    abundances:
        type: uniform
        O: 0.19
        Mg: 0.03
        Si: 0.52
        S: 0.19
        Ar: 0.04
        Ca: 0.03

plasma:
#   initial_t_inner: 10000 K
#   initial_t_rads: 10000 K
    disable_electron_scattering: no
    ionization: lte
    excitation: lte
    #radiative_rates_type – currently supported are lte, nebular and
        detailed
    radiative_rates_type: dilute-blackbody
    #line interaction type – currently supported are scatter,
        downbranch and macroatom
    line_interaction_type: macroatom


montecarlo:
    seed: 23111963
    no_of_packets : 4.0e+4
    iterations: 20

    black_body_sampling:
        start: 1 angstrom
        stop: 1000000 angstrom
        num: 1.e+6
    last_no_of_packets: 1.e+5
    no_of_virtual_packets: 10

    convergence_criteria:
        type: specific
        damping_constant: 1.0
        threshold: 0.05
        fraction: 0.8
        hold: 3
```

```
    t_inner:
        damping_constant: 1.0


spectrum:
    start : 500 angstrom
    stop : 20000 angstrom
    num: 10000
```

References

[1] D. C. Abbott and L. B. Lucy. Multiline transfer and the dynamics of stellar winds. ,
    288:679–693, January 1985.

[2] D. Kasen, R. C. Thomas, and P. Nugent. Time-dependent Monte Carlo Radiative Trans-
    fer Calculations for Three-dimensional Supernova Spectra, Light Curves, and Polariza-
    tion. , 651:366–380, November 2006.

[3] Wolfgang E. Kerzendorf and Stuart A. Sim. A spectral synthesis code for rapid modelling
    of supernovae. 2014.

[4] M. Kromer and S. A. Sim. Time-dependent 3d spectrum synthesis for type ia supernovae.
    2009.

[5] L. B. Lucy. Monte Carlo transition probabilities. , 384:725–735, March 2002.

[6] L. B. Lucy. Monte Carlo transition probabilities. II. , 403:261–275, May 2003.

[7] K. Nomoto, F.-K. Thielemann, and S. Miyaji. The triple alpha reaction at low temper-
    atures in accreting white dwarfs and neutron stars. *Max Planck Institut fur Astrophysik
    Report*, 171, 1984.

[8] K. Nomoto, F.-K. Thielemann, and K. Yokoi. Accreting white dwarf models of Type I
    supernovae. III - Carbon deflagration supernovae. , 286:644–658, November 1984.

[9] R. C. Thomas, P. E. Nugent, and J. C. Meza. SYNAPPS: Data-Driven Analysis for
    Supernova Spectroscopy. , 123:237–248, February 2011.